

Novel *MYCBP::EHD2* and *RUNX1::ZNF780A* Fusion Genes in T-cell Acute Lymphoblastic Leukemia

IOANNIS PANAGOPOULOS¹, KRISTIN ANDERSEN¹, INGA MARIA RINVOLL JOHANNSDOTTIR²,
FRANCESCA MICCI¹ and SVERRE HEIM¹

¹Section for Cancer Cytogenetics, Institute for Cancer Genetics and Informatics,
The Norwegian Radium Hospital, Oslo University Hospital, Oslo, Norway;

²Department of Pediatric Hematology and Oncology, Oslo University Hospital Rikshospitalet, Oslo, Norway

Abstract. *Background/Aim:* T-cell acute lymphoblastic leukemia (T-ALL) is a rare malignancy characterized by proliferation of early T-cell precursors that replace normal hematopoietic cells. T-ALL cells carry non-random chromosome aberrations, fusion genes, and gene mutations, often of prognostic significance. We herein report the genetic findings in cells from a T-ALL patient. *Materials and Methods:* Bone marrow cells from a patient with T-ALL were examined using G-banding, array comparative genomic hybridization (aCGH), RNA sequencing, reverse transcription polymerase chain reaction (RT-PCR), Sanger sequencing, and fluorescence in situ hybridization. *Results:* G-banding revealed *del(1)(p34)*, *add(5)(q14)*, trisomy 8, and monosomy 21 in the leukemic cells. aCGH detected the gross unbalances inferred from the karyotyping results, except that heterozygous loss of chromosome 21 did not include its distal part; *21q22.12-q22.3* was undeleted. In addition, aCGH detected a submicroscopic interstitial 7.56 Mbp deletion in the q arm of chromosome 19 from *19q13.2* to *19q13.33*. RNA sequencing detected and RT-PCR/Sanger sequencing confirmed the presence of two novel chimeras, *MYCBP::EHD2* and *RUNX1::ZNF780A*. They were generated from rearrangements involving subbands *1p34.3* (*MYCBP*), *19q13.2* (*ZNF780A*), *19q13.33* (*EHD2*), and

21q22.12 (*RUNX1*), i.e., at the breakpoints of chromosomal deletions. *Conclusion:* The leukemic cells showed the heterozygous loss of many genes as well as the generation of *MYCBP::EHD2* and *RUNX1::ZNF780A* chimeras. Because the partner genes in the chimeras were found at the breakpoints of the chromosomal deletions, we believe that both the heterozygous losses and the generation of the two chimeras occurred simultaneously, and that they were pathogenetically important.

T-cell acute lymphoblastic leukemia (T-ALL) is a rare malignant disease that accounts for 10-15% of pediatric ALL and 25% of adult ALL. The leukemia is characterized by proliferation of early T-cell precursors replacing the normal hematopoietic cells (1-3). Cytogenetic examination of T-ALL cells has shown that they carry non-random numerical and/or structural chromosome aberrations (this is also typical in other leukemias) that are of diagnostic as well as prognostic importance (4, 5). Molecular investigations of some of these aberrations has led to the identification of recurrent fusion genes (5) and unraveled their role in leukemogenesis. In recent years, utilization of high throughput sequencing technology on T-ALLs has revealed also numerous other fusion genes and gene mutations (6-9). The combined use of high throughput sequencing, mainly transcriptome sequencing, and karyotyping has detected specific fusion genes of unquestionable pathogenetic significance (10-16).

In the present study, we applied the above-mentioned methodological combination on a T-ALL searching for fusion genes.

Materials and Methods

Ethics statement. The study was approved by the regional ethics committee (Regional komité for medisinsk forskningsetikk Sør-Øst, Norge, <http://helseforskning.etikkom.no>, REK: 19178). Written informed consent was obtained from the patient prior to publication of case details. The ethics committee's approval included a review of the consent procedure. All patient information has been de-identified.

Correspondence to: Ioannis Panagopoulos, Section for Cancer Cytogenetics, Institute for Cancer Genetics and Informatics, The Norwegian Radium Hospital, Oslo University Hospital, P.O. Box 4953, Nydalen, NO-0424 Oslo, Norway. Tel: +47 22934424, e-mail: ioannis.panagopoulos@rr-research.no

Key Words: T-cell acute lymphoblastic leukemia, fusion gene, cytogenetics, *MYCBP*, *EHD2*, *RUNX1*, *ZNF780A*, *MYCBP::EHD2*, *RUNX1::ZNF780A*, RNA-sequencing.



This article is an open access article distributed under the terms and conditions of the Creative Commons Attribution (CC BY-NC-ND) 4.0 international license (<https://creativecommons.org/licenses/by-nc-nd/4.0>).

Case report. The patient was a previously healthy 17-year-old boy, admitted to the hospital due to symptoms of upper respiratory tract infection, dysphagia, and an enlarged supraclavicular lymph node. CT-scan of the thorax revealed a tumour in the anterior mediastinum, measuring nine centimetres in the largest diameter. Biopsies from bone marrow and lymph node confirmed an early precursor T-cell leukaemia. He started treatment according to the ALLTogether protocol (17) [ALLTogether1 – A Treatment study protocol of the ALLTogether Consortium for children and young adults (0-45 years of age) with newly diagnosed acute lymphoblastic leukaemia (ALL)], with a slow response and was stratified to the high-risk group. During his treatment he developed pancreatitis and polyneuropathy. He went through a bone marrow transplantation seven months post-diagnosis and is still in remission 1.5 years later.

G-banding and karyotyping. Bone marrow cells obtained at diagnosis were cytogenetically investigated (18, 19). Chromosome preparations were made from metaphase cells of a 24 h culture; they were G-banded using Leishman stain, and karyotyped according to the guidelines of the international system for human cytogenomic nomenclature (2020) (20).

DNA and RNA isolation and complementary DNA (cDNA) synthesis. Genomic DNA and total RNA were extracted from the patient's bone marrow samples at diagnosis. DNA was extracted using the Maxwell 16 Instrument System and the Maxwell 16 Cell DNA Purification Kit (Promega, Madison, WI, USA) and the concentration was measured with a Quantus fluorometer (Promega). Total RNA was extracted using the miRNeasy Mini Kit (Qiagen, Hilden, Germany) and the QiaCube automated purification system according to the manufacturer's instructions (Qiagen); the concentration was measured with the QIAxpert microfluidic UV/VIS spectrophotometer (Qiagen). The Agilent 2100 bioanalyzer and RNA Integrity Number (RIN) were used to assess RNA quality (21). RIN of RNA was 6.6. cDNA was synthesized from one µg of total RNA using the iScript Advanced cDNA Synthesis Kit for RT-qPCR according to the manufacturer's instructions (Bio-Rad, Hercules, CA, USA). The quality of the cDNA synthesis was assessed by amplification of a cDNA fragment of the ABL protooncogene 1, non-receptor tyrosine kinase (*ABL1*) gene using the primer combination ABL1-91F1/ABL1-404R1 (Table I) (22, 23).

Array comparative genomic hybridization (aCGH) analysis. aCGH was performed using the CytoSure array products (Oxford Gene Technology, Begbroke, Oxfordshire, UK) following the company's protocols (14). The reference DNA was Promega's human genomic male DNA (Promega). The slides (CytoSure Cancer +SNP array) were scanned in an Agilent SureScan Dx microarray scanner using Agilent Feature Extraction Software (version 12.1.1.1). Data were analyzed using the CytoSure Interpret analysis software (version 4.9.40). Annotations are based on human genome build 19.

RNA sequencing. High-throughput paired-end RNA-sequencing was performed at the Genomics Core Facility, Norwegian Radium Hospital, Oslo University Hospital (<http://genomics.no/oslo/>). The software FusionCatcher was used to find fusion transcripts (24).

PCR and Sanger sequencing analyses. The primers used for PCR amplification and Sanger sequencing are listed in Table I. The methods involved in PCR amplification and cycle Sanger sequencing have been described in detail in our previous studies (13, 14, 22, 23, 25, 26). Sequence analyses were performed on the Applied Biosystems

SeqStudio Genetic Analyzer system (ThermoFisher Scientific). The basic local alignment search tool (BLAST) software (<https://blast.ncbi.nlm.nih.gov/Blast.cgi>) was used for computer analysis of sequence data (27). The BLAT alignment tool and the human genome browser at UCSC were also used to map the sequences on the Human GRCh37/hg19 assembly (28, 29).

Fluorescence in situ hybridization (FISH) analysis. FISH analysis was performed on metaphase plates using in-house prepared probes made from commercially available bacterial artificial chromosomes (BAC), purchased from the BACPAC Resource Center operated by BACPAC Genomics, Emeryville, CA, USA (<https://bacpacresources.org/>) (Table II). BAC DNAs and labeling of the probes were prepared as previously described (30-32). Probes were labelled with Texas Red-5-dCTP (PerkinElmer, Boston, MA, USA) to obtain a red signal and fluorescein-12-dCTP (PerkinElmer) to obtain a green signal. Chromosome preparations were counterstained with 0.2 µg/ml 4',6-diamidino-2-phenylindole and overlaid with a 24x50 mm² coverslip. Fluorescent signals were captured and analyzed using the CytoVision system (Leica Biosystems, Newcastle, UK). Mapping of the clones on normal controls was performed to confirm their chromosomal location (Table II).

Results

Cytogenetics and aCGH analyses. Cytogenetic examination of short-term cultured cells from the patient's bone marrow revealed a deletion on the p arm of chromosome 1, an addition of extra material of unknown chromosomal origin on the long arm of chromosome 5, a gain of chromosome 8, and loss of one chromosome 21 on 6 out of 10 examined metaphases (Figure 1). Consequently, the karyotype was: 46,XY,del(1)(p34),add(5)(q14),+8,-21[6]/46,XY[4].

The results from aCGH are shown in Figure 2, Figure 3, Figure 4, Figure 5 and Figure 6. aCGH confirmed the del(1)(p34), revealing that the breakpoint was in the subband 1p34.3, in the area hosting the genes Ras related GTP binding C (*RRAGC*), MYC binding protein (*MYCBP*), gap junction protein alpha 9 (*GJA9*) and rhomboid like 2 (*RHBDL2*) (Figure 2, Figure 3A and B). Because there were no probes on *MYCBP* and *GJA9*, the breakpoint could not map more precisely (Figure 3B). For chromosome 5, the aCGH analysis showed that the cytogenetically detected add(5)(q14) was accompanied by a deletion which started at 5q14, just downstream of the adhesion G protein-coupled receptor V1 gene (*ADGRV1*, also known as *GRP98*) (Figure 2, Figure 4A and B). Besides confirming the cytogenetically observed trisomy for chromosome 8 (Figure 2), aCGH also detected an interstitial deletion in 19q13 (Figure 2 and Figure 5) that started between the zinc finger protein 780A (*ZNF780A*) and mitogen-activated protein kinase 10 (*MAP3K10*) genes (Figure 5A and B) and ended in EH domain containing 2 (*EHD2*) (Figure 5A and C). Because of the low number of probes at the breakpoint regions, the interstitial deletion in 19q13 could not be mapped more precisely (Figure 5B and C). aCGH also showed loss of a

Table I. Designation, sequence (5'→3'), and position in reference sequences of the forward (F) and reverse (R) primers of the genes *MYC* binding protein (*MYCBP*), *EH* domain containing 2 (*EHD2*), *RUNX* family transcription factor 1 (*RUNX1*) and zinc finger protein 780A (*ZNF780A*), which were used for polymerase chain reaction amplification and Sanger sequencing analyses. For Sanger sequencing analyses the forward primers had the M13 forward primer sequence TGTAACGACGGCCAGT at their 5'-end. The reverse primers had the M13 reverse primer sequence CAGGAAACAGCTATGACC at their 5'-end.

Designation	Method	Sequence (5'→3')	Reference sequence: Position
MYCBP-199F1	PCR/Sanger sequencing	AGGAGCTGCTACTCCAGAAAATCCA	NM_012333.5: 199-223
MYCBP-217F1	Sanger sequencing	AAATCCAGAAATAGAGCTGCTTCGC	NM_012333.5: 217-241
EHD2-1197R1	PCR/ Sanger sequencing	GGGAGATGTGATGTTCCAGCTGAA	NM_014601.4: 1220-1197
EHD2-1163R1	Sanger sequencing	ATGACGGGCAGTTTGAGGATCAG	NM_014601.4: 1185-1163
RUNX1-155F1	PCR/Sanger sequencing	CGCCTTCAGAAGAGGGTGCATT	NM_001754.4: 155-176
RUNX1-175F1	Sanger sequencing	TTTTTCAGGAGGAAGCGATGGCT	NM_001754.4: 175-196
ZNF780A-199R1	PCR/Sanger sequencing	GGCACTCCCCTCCTCTGAGA	NM_001142577.2: 220-199
ZNF780A-173R1	Sanger sequencing	TCAATGGCCACATCCCTGAATG	NM_001142577.2: 194-173

Table II. BAC probes used for fluorescence in situ hybridization (FISH) experiments in order to detect the *MYCBP::EHD2* chimera. The position of the *MYCB* and *EHD2* genes is also given.

BAC clones	Accession number	Chromosome mapping	Targeted gene	Position on GRCh38/hg38 assembly	Labelling
RP11-334L9	AL354702.7	1p34.3	<i>MYCBP</i>	chr1:38680478-38785899	Red
RP11-445L12	AL714019.7	1p34.3	<i>MYCBP</i>	chr1:38939038-38957512	Red
	BZ894067			chr1:38825185-39022139	
	BZ774593				
	NM_012333.5	1p34.3	<i>MYCBP</i>	chr1:38862493-38873348	
RP11-781D11	AL606465.21	1p34.3	<i>MYCBP</i>	chr1:38957513-39071615	Red
RP11-105H7	AQ323479.1	19q13.33	<i>EHD2</i>	chr19:47520752-47703222	Green
	AQ323477.1				
RP11-927F22	AQ770965.1	19q13.33	<i>EHD2</i>	chr19:47664339-47836162	Green
	AQ666010.1				
	NM_014601.4	19q13.33	<i>EHD2</i>	chr19:47713422-47743134	
RP11-108F6	AQ348867.1	19q13.33	<i>EHD2</i>	chr19:47788899-47919546	Green
	AQ319155.1				
RP11-1201N3	AC124853.2	19q13.33	<i>EHD2</i>	chr19:47886351-47966569	Green

large part of chromosome 21 (21p11.2-q22.2) (Figure 2, Figure 6A and B). However, 21q22.12-q22.3, including exons 1 and 2 of *RUNX1*, was not deleted (Figure 6B).

RNA sequencing, RT-PCR, and Sanger sequencing analyses. Analysis of raw sequencing data using FusionCatcher detected two fusion transcripts. The first transcript was a fusion of exon 4 of *MYCBP* from 1p34.4 (nucleotide 310 in reference sequence NM_012333.5) with exon 5 of *EHD2* from 19q13.33 (nucleotide 1088 in reference sequence NM_014601.4): AAGAGAAGTATGAAGCTATTGTAGAAGAAAATAAAAA ACTGAAAGCAAAG::GTTTCACGCTTACATCATCAGCTA CCTGAAGAAGGAGATGCCCTCTGTGTT. The second chimeric transcript was a fusion of exon 2 of *RUNX1* from 21q22.12 (nucleotide 248 in reference sequence NM_001754.4) with exon 3 of *ZNF780A* from 19q13.2

(nucleotide 109 in reference sequence NM_001142577.2): AGACAGCATATTTGAGTCATTTCTTCGTACCCACAGT GCTTCATGAGAG::GGGAGAAGCCCGAGGAAGATTGA CCAGTTTTGTAATTCTAGCAACATGGT.

RT-PCR using the MYCBP-199F1 and EHD2-1197R1 primer combination amplified a 245 bp cDNA fragment which was shown by Sanger sequencing to confirm the *MYCBP::EHD2* fusion transcript detected by the RNA sequencing/FusionCatcher analysis (Figure 7A). RT-PCR with RUNX1-155F1 and ZNF780A-199R1 primers amplified a 206 bp fragment, which confirmed (by Sanger sequencing) the *RUNX1::ZNF780A* fusion transcript detected by the RNA sequencing/FusionCatcher (Figure 7B).

Fluorescence in situ hybridization (FISH) analyses. FISH analysis on metaphase plates using in-house prepared probes

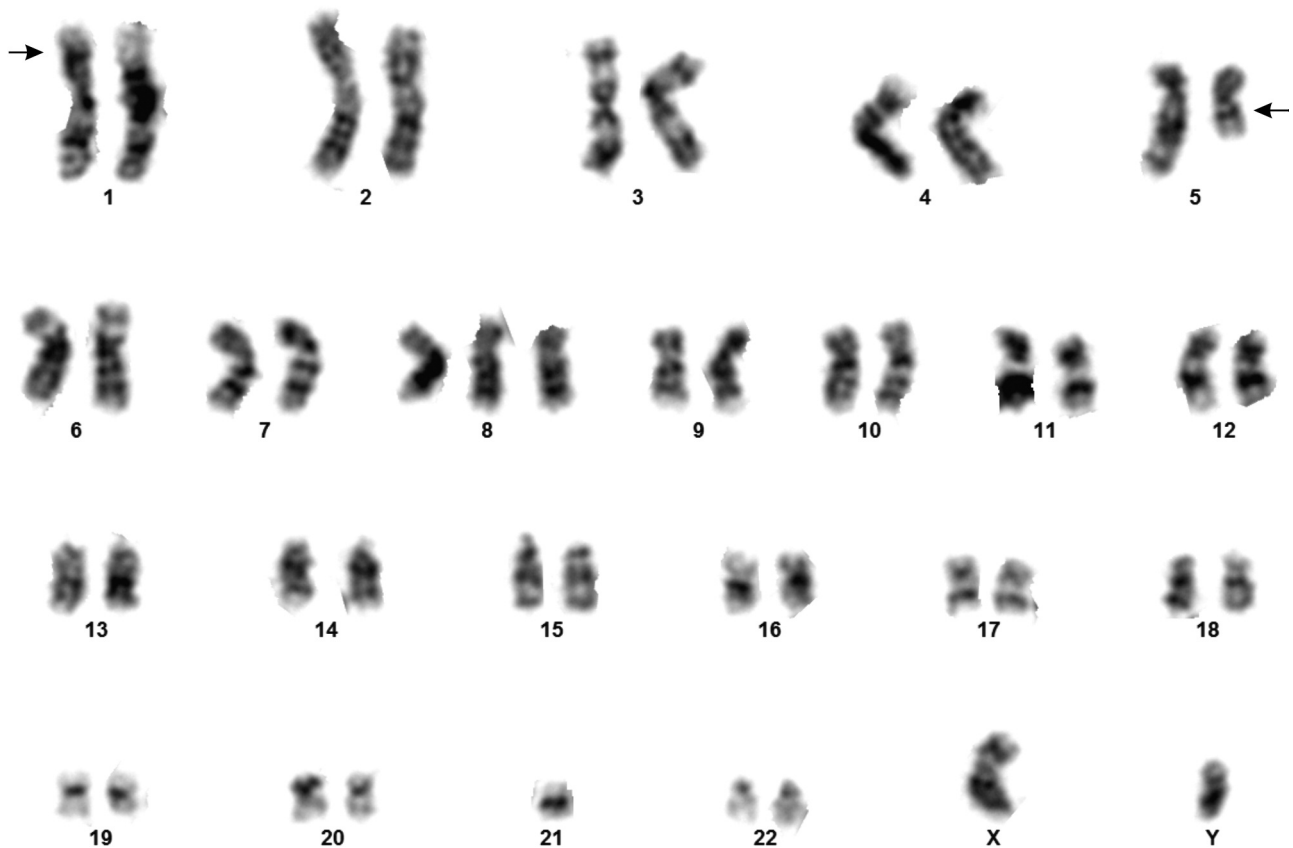


Figure 1. G-banding analysis of the bone marrow cells of the T-ALL patient. A karyogram is shown, depicting the chromosome aberrations of the leukemic cells corresponding to the karyotype 46,XY,del(1)(p34),add(5)(q14),+8,-21. Arrows indicate breakpoints.

for the *MYCBP* (red labeled) and *EHD2* (green label) genes showed a red signal corresponding to a normal *MYCBP* on chromosome 1, a green signal on normal chromosome 19 corresponding to *EHD2*, a fusion red/green signal on der(1) chromosome corresponding to a *MYCBP::EHD2* chimera, and a red signal on der(19) indicating that material from chromosome band 1p34 had been moved to band q13 of the der(19) (Figure 7C).

Discussion

As a consequence of the chromosomal aberrations, there was heterozygous loss of many genes on chromosomes 1, 5, 19 and 21, due to the del(1)(p34), add(5)(q14), interstitial deletion on 19q, and deletion of a large part of chromosome 21, found by aCGH and/or G-banding. Trisomy 8 was also part of the karyotype; this aberration is common in leukemia(s) both as the sole abnormality and as a secondary change, although its exact role in leukemogenesis remains enigmatic (33-35). In the Mitelman database of chromosome

aberrations and gene fusions in cancer (last updated on July 27, 2022), only 245 out of 3225 (7.6%) T-cell lineage acute lymphoblastic leukemia/lymphoblastic lymphoma entries have been reported with +8 in their karyotype. In most of them, the +8 was a secondary aberration (33).

In addition to genomic imbalances, the cytogenetic aberrations also resulted in generation of the *MYCBP::EHD2* and *RUNX1::ZNF780A* chimeras, since the partner genes of both were found at the breakpoints of the chromosomal rearrangements. Thus, *MYCBP::EHD2* is the product of recombination of one gene in 1p34 (*MYCBP*), visibly affected as a del(1)(p34), and another in the q13.33 subband (*EHD2*), affected by the interstitial deletion of chromosome 19, whereas the *RUNX1::ZNF780A* chimera is a product of the deletion of chromosome 21 and the proximal breakpoint of the 19q13.2. To the best of our knowledge, this is the first time that these fusion genes, *i.e.* *MYCBP::EHD2* and *RUNX1::ZNF780A*, are described.

MYCBP codes for a protein which binds to the N-terminal transactivation domain of MYC, enhancing the latter

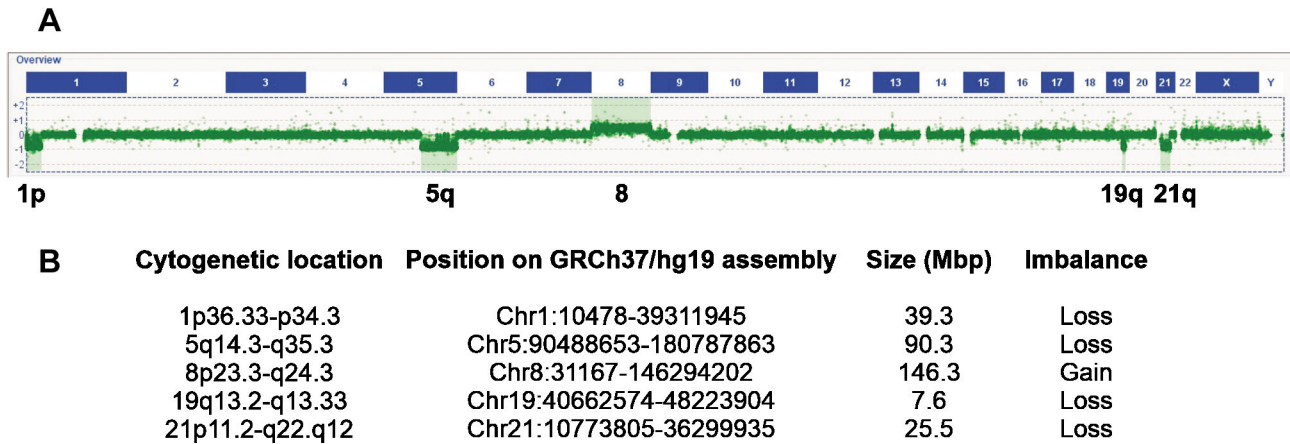


Figure 2. Array comparative genomic hybridization (aCGH) examination of the bone marrow cells of the T-ALL patient. (A) Genetic profile of whole genome showing trisomy for chromosome 8 and losses from parts of chromosomes 1, 5, 19, and 21. (B) The cytogenetic location, position on GRCh37/hg19 assembly, size (in Mbp), and gain/loss of the genetic imbalances are presented.

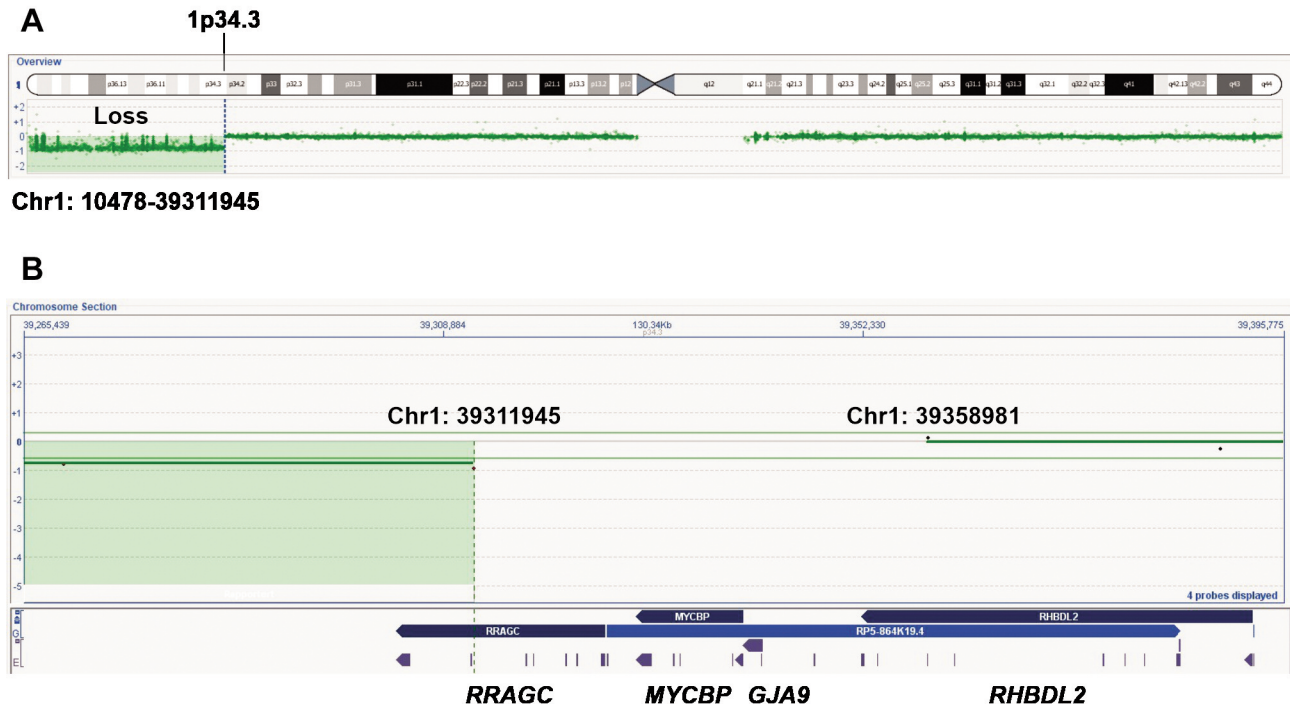


Figure 3. aCGH showing the deleted part of the p arm of chromosome 1. (A) Based on the hg19 assembly the deletion ended at position chr1:39311945, on the subband 1p34.3. The most distal (p-telomeric) probe in the assay mapped at position chr1:10478. (B) The area at position chr1:39311945 hosting the genes *Ras* related GTP binding C (*RRAGC*), *MYC* binding protein (*MYCBP*), gap junction protein alpha 9 (*GJA9*) and rhomboid like 2 (*RHBDL2*). Because there were no probes on *MYCBP* and *GJA9*, the breakpoint could not map more precisely. Highlights indicate the deleted (loss) part.

protein's transcriptional activation ability (36). *MYCBP* was also found to interact with the A kinase anchoring proteins *AKAP1* and *AKAP8* (37, 38) as well as ADP ribosylation factor guanine nucleotide exchange factors 1 and 2

(*ARFGEF1* and *ARFGEF2*), which play important roles in intracellular vesicular trafficking (39). Because the promoter of *MYCBP* contains binding sites for the lymphoid enhancer binding factor 1 (*LEF1*), *MYCBP* expression can be

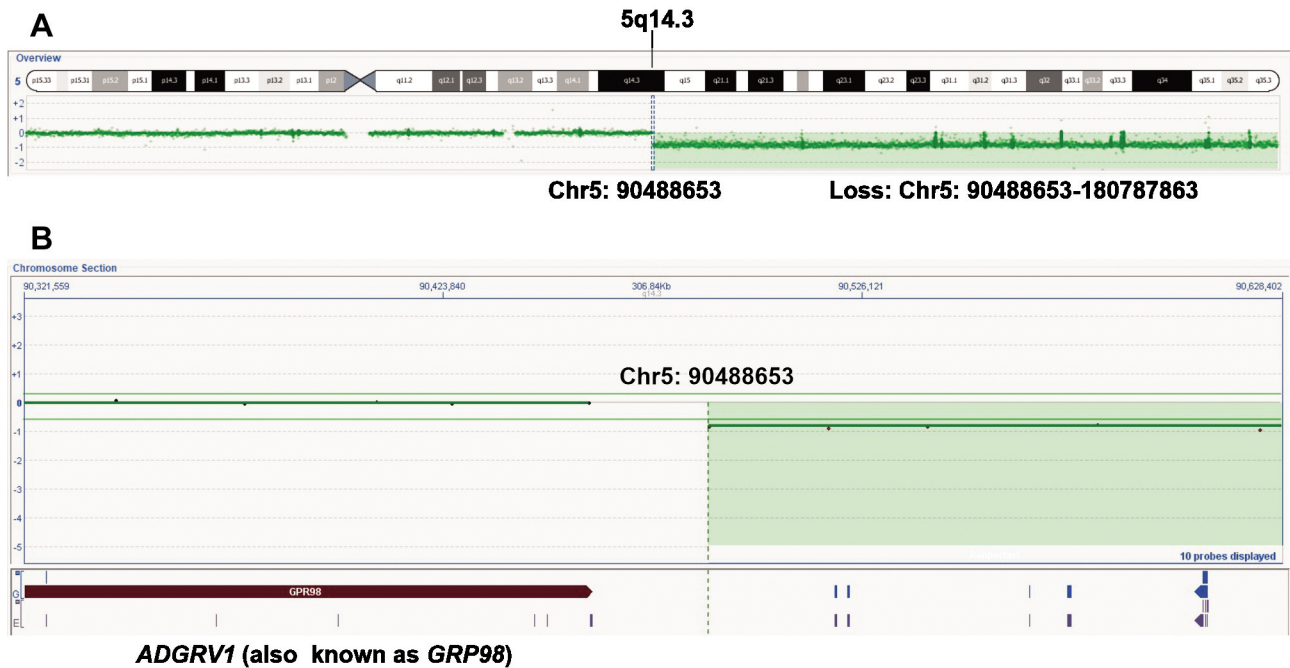


Figure 4. aCGH showing the deleted part of the q arm of chromosome 5. (A) The deletion started at position chr5:90488653 on the subband 5q14.3 and ended on subband 5q35.3. The most distal (q-telomeric) probe in the assay mapped at position chr5: 180787863. (B) The area at position chr5:90488653 shows that the deletion is just downstream of the adhesion G protein-coupled receptor V1 gene (ADGRV1, also known as GRP98). Highlights indicate the deleted (loss) part.

regulated through the beta-catenin/LEF1 pathway (40). *LEF1* (on 4q25) is highly expressed in T-cells (41, 42). In lower grade gliomas, loss of *MYCBP* was found to be associated with an improved survival (43). *MYCBP* is involved in proliferation, migration, and invasion of colorectal cancer (44) and in progression of lung adenocarcinoma (45).

The four paralogue genes *EHD1* (chromosome subband 11q13.1), *EHD2* (19q13.33), *EHD3* (2p23.1), and *EHD4* (15q15.1) code for Eps15 homology domain (EHD) proteins involved in the regulation of endocytic trafficking but in separate subcellular locations (46-49). At the N terminus, the EHD proteins contain a nucleotide-binding consensus site whereas at the C-terminus, they have an EF-hand calcium-binding EHD domain which interacts with proteins through binding to NPF motifs (46-50). According to the model proposed by Naslavsky and Caplan (49), “cytoplasmic localized EHD proteins bind ATP and dimerize. EHD dimerization causes the formation of a membrane binding site and the EHD proteins associate with tubular membranes, where they undergo further oligomerization. Upon ATP hydrolysis, the membranes are destabilized, leading to scission of vesicles containing concentrated cargo/receptors, thus facilitating vesicular transport”.

EHD2 has been found to be located in the inner leaflet of plasma membrane where it may interact with the actin

cytoskeleton and bind to EHP1 protein through its N-terminal and C-terminal EH domains (51). This interaction indicates that *EHD2* may be involved in clathrin-dependent endocytosis to actin and endosome recycling (50-54). *EHD2* has also been found to interact with the proteins GLUT4, AP-1 subunit $\mu 1$, AP-2 subunit $\mu 2$, CALM, Rabenosyn-5, Myoferlin and prohibitin (48-50) and to be able to enter the nucleus where it represses transcription (55).

Based on the reference sequences NM_012333.5/NP_036465.2 and NM_014601.4/NP_055416.2 for the genes *MYCBP* and *EHD2*, respectively, the *MYCBP::EHD2* chimera was predicted to code for a 327 amino acid chimeric peptide consisting of the first 89 amino acids of MYCB and the last 238 of *EHD2* (amino acids 307-543 in NP_055416.2). Thus, it would contain the N-terminal part of *MYCBP* which increases the transcription activity of MYC, and the part of *EHD2* protein which contains the bipartite nuclear localization signal, the membrane binding region, nuclear export signal, and the EHD domain at the C-terminus (Figure 8). Two algorithms for prediction of eukaryotic protein subcellular localization, PSORT II and DeepLoc-2.0, predict that *MYCBP::EHD2* is a cytoplasmic protein (56, 57). However, functional studies are needed to determine the role of *MYCBP::EHD2* in leukemogenesis.

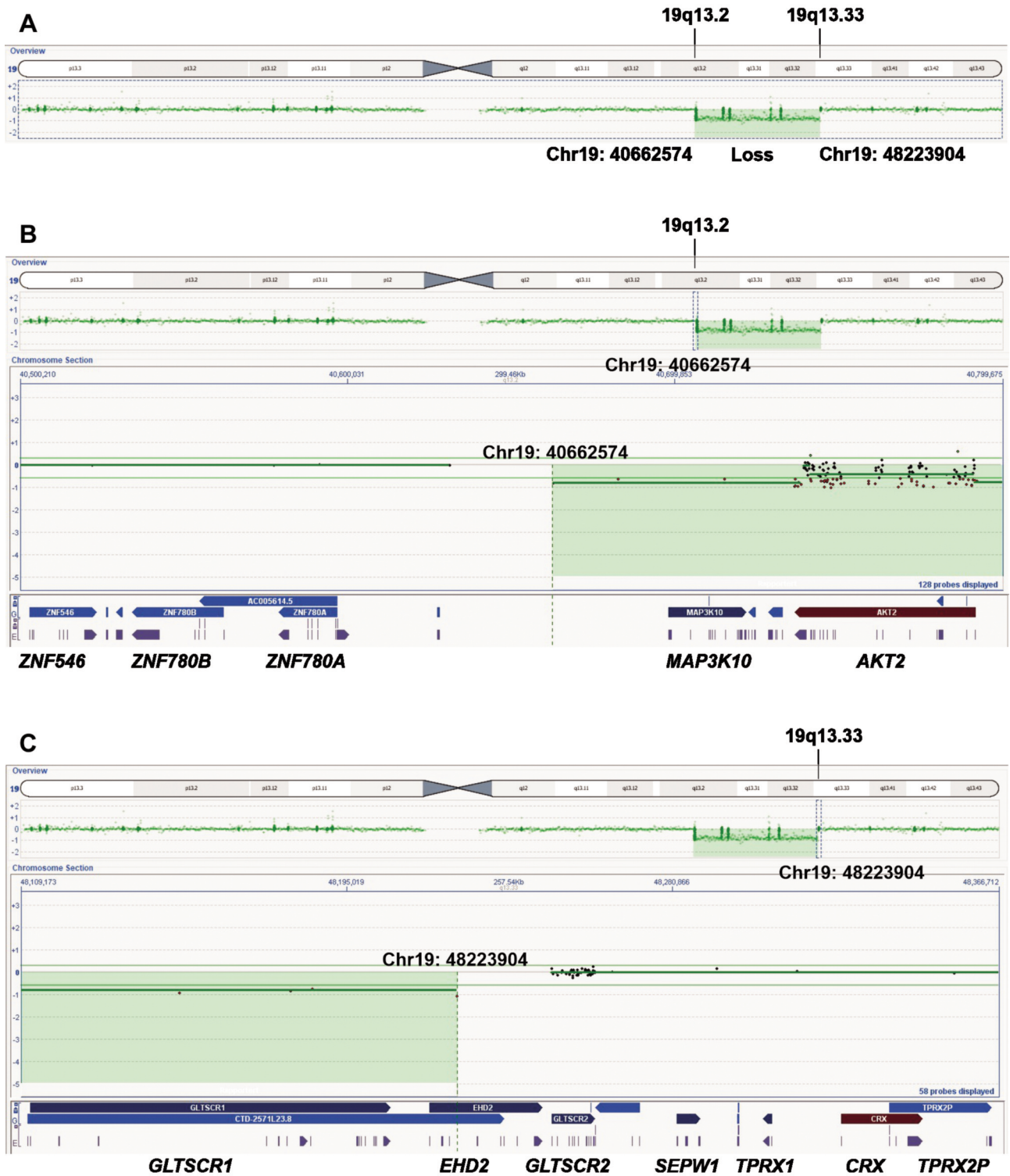


Figure 5. aCGH analysis showing the interstitial deletion in *q* arm of chromosome 19. (A) Genetic profile of whole chromosome 19 showing the deletion started at position Chr19:40662574 on subband 19q13.2 and ended at chr19: 48223904 on subband 19q13.33. (B) The area at position Chr19:40662574 showing that the deletion started between the genes zinc finger protein 780A (ZNF780A) and mitogen-activated protein kinase 10 (MAP3K10). (C) The area at position chr19: 48223904 showing that deletion ended within the EH domain containing 2 (EHD2) gene. Because of the low number of probes at the breakpoint regions, the interstitial deletion in 19q13 could not be mapped more precisely. Highlights indicate the deleted (loss) part.

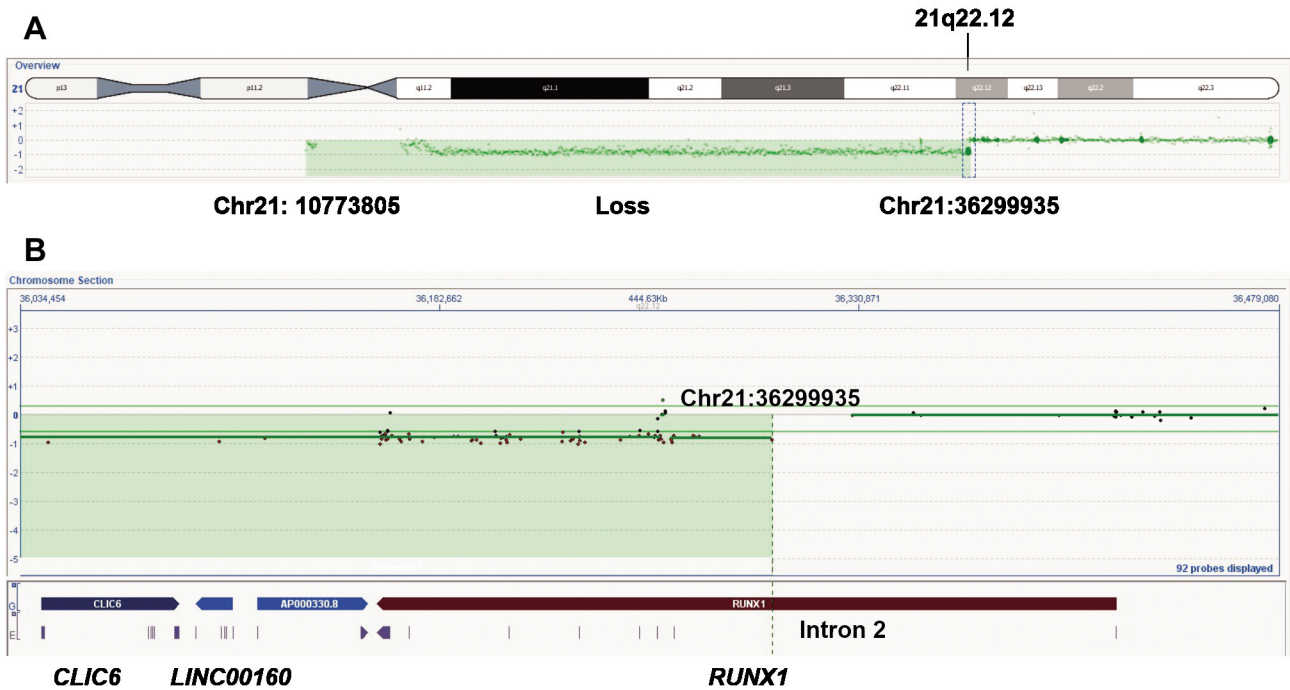


Figure 6. aCGH analysis showing the deleted part of chromosome 21. (A) The deletion ended at position Chr21: 36299935 on the subband 21q22.13. The most distal probe on the p arm of chromosome 21 in the assay mapped at position Chr21:10773805. (B) The area at position Chr21: 36299935 showing that the deletion ended within intron 2 of RUNX1.

Based on the reference sequences NM_001754.4/NP_001745.2 and NM_001142577.2/NP_001136049.1 for the genes *RUNX1* and *ZNF780A*, the *RUNX1::ZNF780A* chimera does not result in a chimeric protein but instead, the entire coding region of *ZNF780A* comes under the control of the distal P1 promoter of *RUNX1* (58-60). Expression of *RUNX1* is driven by two alternative promoters, a proximal (P2) and a distal one (P1) (58-60). The P2 promoter is active in brain, liver, lung, kidney, heart and pancreatic tissue and drives the expression of transcript variant 2 of *RUNX1* (reference sequence: NM_001001890.3) which produces the RUNX1b isoform (reference sequence NP_001001890.1, also known as AML1b) (58, 61, 62). The P1 promoter is predominantly functional in hematopoietic stem cells, megakaryocytes, as well as T lymphocytes in the thymus and spleen; it is a direct target of Wnt/ β -catenin signaling and drives the expression of transcript variant 1 of *RUNX1* (reference sequence NM_001754.4), which is translated to the RUNX1c isoform protein (NP_001745.2, also known as isoform AML1c) (60, 62-66). Exon 1 of transcript variant 1 of *RUNX1* is a non-coding region whereas exon 2 codes for MASDSIFESFPSYPQCFMR which is out of frame with *ZNF780A* (58-62). The *ZNF780A* gene codes for a zinc finger transcription factor, located in the nucleus, which contains a krueppel associated box domain, two double zinc-finger domains, a region with multiple C2H2 zinc

fingers, and multiple DNA-binding sites (https://www.ncbi.nlm.nih.gov/protein/NP_001136049.1). It was found to have prognostic and predictive value for hepatocellular carcinoma together with fourteen others transcription factors (67). Recently, recurrent *ZNF780A* mutations were reported in myxofibrosarcomas (68). The exact cellular function of *ZNF780A* and its role in the development and progression of neoplasms are currently unknown.

Conclusion

In conclusion, we used in the present study G-banding, aCGH, RNA sequencing, RT-PCR/Sanger sequencing and FISH to identify both heterozygous losses and generation of two fusion genes, *MYCBP::EHD2* and *RUNX1::ZNF780A*, in bone marrow cells from a 17-year-old boy with T-ALL. Because the partner genes in the two chimeras were found at the breakpoints of the chromosomal deletion, we believe that both the heterozygous loss(es) and the generation of the two chimeras occurred simultaneously, and that they were pathogenetically important.

Conflicts of Interest

The Authors declare that they have no potential conflicts of interest.

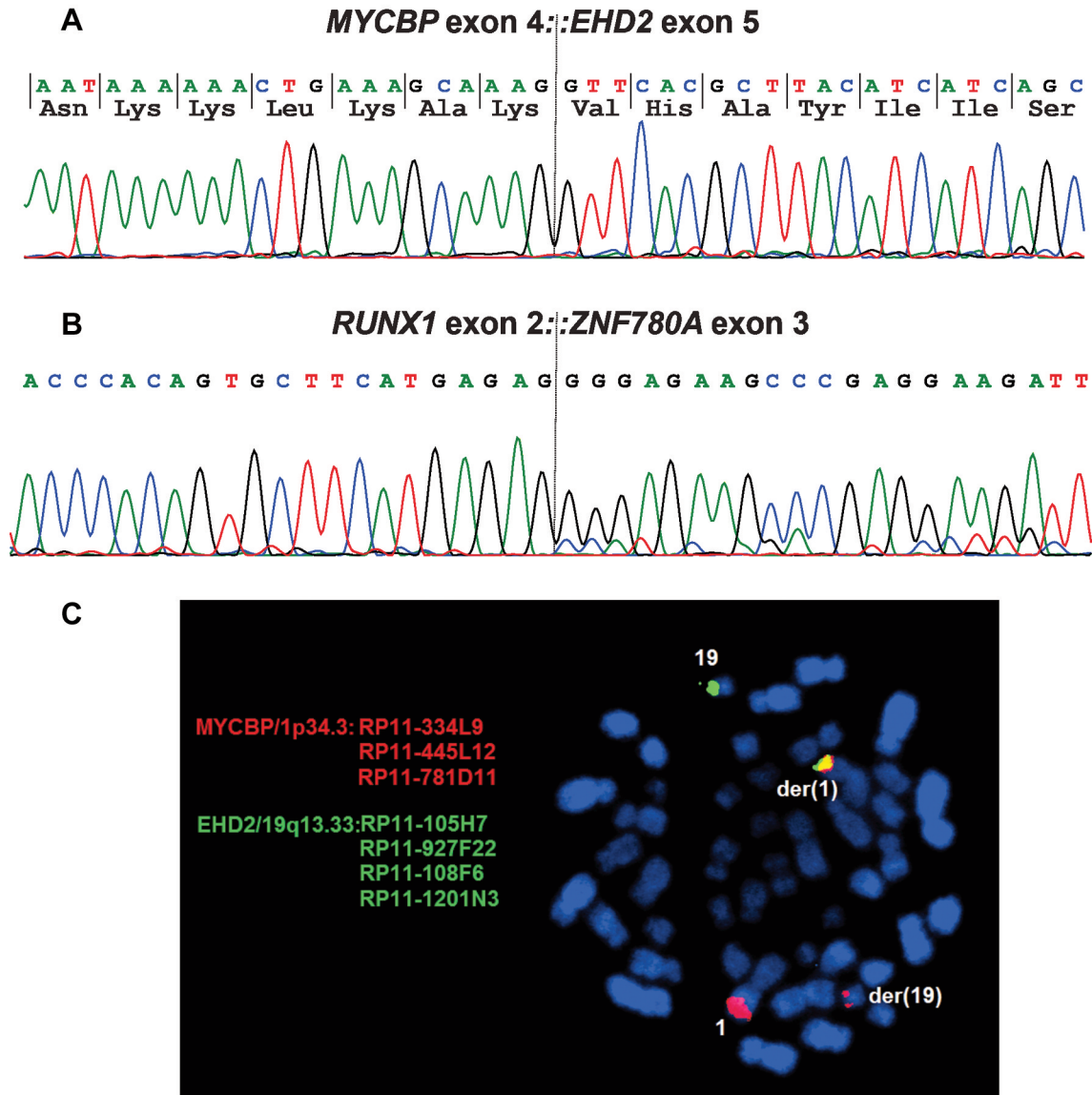


Figure 7. Sanger sequencing and fluorescence in situ hybridization (FISH) of the bone marrow cells of the T-ALL patient. (A) Partial Sanger sequencing chromatogram showing the junction between exon 4 of MYCBP and exon 2 of EHD2. (B) Partial Sanger sequencing chromatogram showing the junction between exon 2 of RUNX1 and exon 3 of ZNF780A. (C) FISH analysis on metaphase plates using in-house prepared probes for the MYCBP (red labeled) and EHD2 (green label) genes showed a red signal corresponding to normal MYCBP on chromosome 1, a green signal on normal chromosome 19 corresponding to EHD2, a fusion red/green signal on der(1) chromosome which corresponded to the MYCBP::EHD2 chimera, and a red signal on der(19) indicating that material from chromosome bad 1p34 translocated to q13 of der(19).

Authors' Contributions

IP designed and supervised the research, performed molecular genetic experiments, the bioinformatics analysis, and wrote the manuscript. KA performed molecular genetic experiments and interpreted the data. IMRJ made clinical evaluations and treated the patient. FM evaluated the data. SH assisted with experimental design and writing of the manuscript. All Authors read and approved of the final manuscript.

Acknowledgements

This study was supported by grants from Radiumhospitalets Legater.

References

- 1 Raetz EA and Teachey DT: T-cell acute lymphoblastic leukemia. *Hematology Am Soc Hematol Educ Program* 2016(1): 580-588, 2016. PMID: 27913532. DOI: 10.1182/asheducation-2016.1.580

```

atg gcc cat tac aaa gcc gcc gac tcg aag cgt gag cag ttc cgg agg tac ttg gag aag
M  A  H  Y  K  A  A  D  S  K  R  E  Q  F  R  R  Y  L  E  K
tcg ggg gtg ctg gac acg ctg acc aag gtg ttg gta gcc tta tat gaa gaa cca gag aaa
S  G  V  L  D  T  L  T  K  V  L  V  A  L  Y  E  E  P  E  K
cct aac agt gct ttg gat ttt tta aag cat cac tta gga gct gct act cca gaa aat cca
P  N  S  A  L  D  F  L  K  H  H  L  G  A  A  T  P  E  N  P
gaa ata gag ctg ctt cgc cta gaa ctg gcc gaa atg aaa gag aag tat gaa gct att gta
E  I  E  L  L  R  L  E  L  A  E  M  K  E  K  Y  E  A  I  V
gaa gaa aat aaa aaa ctg aaa gca aag gtt cac gct tac atc atc agc tac ctg aag aag
E  E  N  K  K  L  K  A  K  V  H  A  Y  I  I  S  Y  L  K  K
gag atg ccc tct gtg ttt ggg aag gag aac aag aag aag cag ctg
E  M  P  S  V  F  G  K  E  N  K  K  K  Q  L  I  L  K  L  P
gtc atc ttt gcg aag att cag ctg gaa cat cac atc tcc cct ggg gac ttt cct gat tgc
V  I  F  A  K  I  Q  L  E  H  H  I  S  P  G  D  F  P  D  C
cag aaa atg cag gag ctg ctg atg gcg cac gac ttc acc aag ttt cac tcg ctg aag ccg
Q  K  M  Q  E  L  L  M  A  H  D  F  T  K  F  H  S  L  K  P
aag ctg cta gag gca ctg gac gag atg ctg acg cac gac atc gcc aag ctc atg ccc ctg
K  L  L  E  A  L  D  E  M  L  T  H  D  I  A  K  L  M  P  L
ctg cgg cag gag gag ctg gag agc acc gag gtg ggc gtg cag ggg ggc gct ttt gag ggc
L  R  Q  E  E  L  E  S  T  E  V  G  V  Q  G  A  F  E  G
acc cac atg ggc ccg ttt gtg gag cgg gga cct gac gag gcc atg gag gac ggc gag gag
T  H  M  G  P  F  V  E  R  G  P  D  E  A  M  E  D  G  E  E
ggc tcg gac gac gag gcc gag tgg gtg gtg acc aag gac aag tcc aaa tac gac gag atc
G  S  D  D  E  A  E  W  V  V  T  K  D  K  S  K  Y  D  E  I
ttc tac aac ctg gcg cct gcc gac ggc aag ctg agc ggc tcc aag gcc aag acc tgg atg
F  Y  N  L  A  P  A  D  G  K  L  S  G  S  K  A  K  T  W  M
gtg ggg acc aag ctc ccc aac tca gtg ctg ggg cgc atc tgg aag ctc agc gat gtg gac
V  G  T  K  L  P  N  S  V  L  G  R  I  W  K  L  S  D  V  D
cgc gac ggc atg ctg gat gat gag gag ttc gcg ctg gcc agc cac ctc atc gag gcc aag
R  D  G  M  L  D  D  E  E  F  A  L  A  S  H  L  I  E  A  K
ctg gaa ggc cac ggg ctg ccc gcc aac ctg ccc cgt cgc ctg gtg cca ccc tcc aag cga
L  E  G  H  G  L  P  A  N  L  P  R  R  L  V  P  P  S  K  R
cgc cac aag ggc tcc gcc gag tga
R  H  K  G  S  A  E  -

```

Binds to N-terminal part of MYC and stimulates MYC activation

Bipartite nuclear localization signal **Nuclear exit signal** **EF hand motif Eps homology domain**

Figure 8. The coding part of the chimeric MYCBP::EHD2 transcript. MYCBP sequence is shown in grey background. The domain which binds to N-terminal part of MYC and stimulates MYC activation is written with red letters. The nuclear exit signal is shown in light blue background. The EF hand motif and EPS homology domain are written with dark blue and purple letters and are shown in dark yellow background.

- 2 Girardi T, Vicente C, Cools J and De Keersmaecker K: The genetics and molecular biology of T-ALL. *Blood* 129(9): 1113-1123, 2017. PMID: 28115373. DOI: 10.1182/blood-2016-10-706465
- 3 Terwilliger T and Abdul-Hay M: Acute lymphoblastic leukemia: a comprehensive review and 2017 update. *Blood Cancer J* 7(6): e577, 2017. PMID: 28665419. DOI: 10.1038/bcj.2017.53
- 4 Graux C, Cools J, Michaux L, Vandenberghe P and Hagemeijer A: Cytogenetics and molecular genetics of T-cell acute lymphoblastic leukemia: from thymocyte to lymphoblast. *Leukemia* 20(9): 1496-1510, 2006. PMID: 16826225. DOI: 10.1038/sj.leu.2404302
- 5 Heim S and Mitelman F: Cancer cytogenetics: Chromosomal and molecular genetic aberrations of tumor cells. Fourth Edition edn. Wiley-Blackwell, 2015.
- 6 Mullighan CG: The genomic landscape of acute lymphoblastic leukemia in children and young adults. *Hematology Am Soc Hematol Educ Program* 2014(1): 174-180, 2014. PMID: 25696852. DOI: 10.1182/asheducation-2014.1.174
- 7 Liu Y, Easton J, Shao Y, Maciaszek J, Wang Z, Wilkinson MR, McCastlain K, Edmonson M, Pounds SB, Shi L, Zhou X, Ma X, Sioson E, Li Y, Rusch M, Gupta P, Pei D, Cheng C, Smith MA, Auville JG, Gerhard DS, Relling MV, Winick NJ, Carroll AJ,

- Heerema NA, Raetz E, Devidas M, Willman CL, Harvey RC, Carroll WL, Dunsmore KP, Winter SS, Wood BL, Sorrentino BP, Downing JR, Loh ML, Hunger SP, Zhang J and Mullighan CG: The genomic landscape of pediatric and young adult T-lineage acute lymphoblastic leukemia. *Nat Genet* 49(8): 1211-1218, 2017. PMID: 28671688. DOI: 10.1038/ng.3909
- 8 Chen B, Jiang L, Zhong ML, Li JF, Li BS, Peng LJ, Dai YT, Cui BW, Yan TQ, Zhang WN, Weng XQ, Xie YY, Lu J, Ren RB, Chen SN, Hu JD, Wu DP, Chen Z, Tang JY, Huang JY, Mi JQ and Chen SJ: Identification of fusion genes and characterization of transcriptome features in T-cell acute lymphoblastic leukemia. *Proc Natl Acad Sci USA* 115(2): 373-378, 2018. PMID: 29279377. DOI: 10.1073/pnas.1717125115
- 9 Mansur MB, Furness CL, Nakjang S, Enshaei A, Alpar D, Colman SM, Minto L, Irving J, Poole BV, Noronha EP, Savola S, Iqbal S, Gribben J, Pombo-de-Oliveira MS, Ford TM, Greaves MF and van Delft FW: The genomic landscape of teenage and young adult T-cell acute lymphoblastic leukemia. *Cancer Med* 10(14): 4864-4873, 2021. PMID: 34080325. DOI: 10.1002/cam4.4024
- 10 Lu QR, Yuk D, Alberta JA, Zhu Z, Pawlitzky I, Chan J, McMahon AP, Stiles CD and Rowitch DH: Sonic hedgehog—regulated oligodendrocyte lineage genes encoding bHLH proteins in the mammalian central nervous system. *Neuron* 25(2): 317-329, 2000. PMID: 10719888. DOI: 10.1016/s0896-6273(00)80897-1
- 11 Tanas MR, Sboner A, Oliveira AM, Erickson-Johnson MR, Hespelt J, Hanwright PJ, Flanagan J, Luo Y, Fenwick K, Natrajan R, Mitsopoulos C, Zvelebil M, Hoch BL, Weiss SW, Debiec-Rychter M, Sciort R, West RB, Lazar AJ, Ashworth A, Reis-Filho JS, Lord CJ, Gerstein MB, Rubin MA and Rubin BP: Identification of a disease-defining gene fusion in epithelioid hemangioendothelioma. *Sci Transl Med* 3(98): 98ra82, 2011. PMID: 21885404. DOI: 10.1126/scitranslmed.3002409
- 12 Panagopoulos I, Thorsen J, Gorunova L, Micci F and Heim S: Sequential combination of karyotyping and RNA-sequencing in the search for cancer-specific fusion genes. *Int J Biochem Cell Biol* 53: 462-465, 2014. PMID: 24863361. DOI: 10.1016/j.biocel.2014.05.018
- 13 Panagopoulos I, Andersen K, Eilert-Olsen M, Rognlien AG, Munthe-Kaas MC, Micci F and Heim S: Rare *KMT2A-ELL* and novel *ZNF56-KMT2A* fusion genes in pediatric T-cell acute lymphoblastic leukemia. *Cancer Genomics Proteomics* 18(2): 121-131, 2021. PMID: 33608309. DOI: 10.21873/cgp.20247
- 14 Panagopoulos I, Andersen K, Eilert-Olsen M, Zeller B, Munthe-Kaas MC, Buechner J, Osnes LTN, Micci F and Heim S: Therapy-induced deletion in 11q23 leading to fusion of *KMT2A* with *ARHGEF12* and development of B lineage acute lymphoblastic leukemia in a child treated for acute myeloid leukemia caused by t(9;11)(p21;q23)/*KMT2A-MLL3*. *Cancer Genomics Proteomics* 18(1): 67-81, 2021. PMID: 33419897. DOI: 10.21873/cgp.20242
- 15 Panagopoulos I and Heim S: Interstitial deletions generating fusion genes. *Cancer Genomics Proteomics* 18(3): 167-196, 2021. PMID: 33893073. DOI: 10.21873/cgp.20251
- 16 Panagopoulos I and Heim S: Neoplasia-associated chromosome translocations resulting in gene truncation. *Cancer Genomics Proteomics* 19(6): 647-672, 2022. PMID: 36316036. DOI: 10.21873/cgp.20349
- 17 EU Clinical Trials Register: ALLTogether1— A treatment study protocol of the ALLTogether Consortium for children and young adults (0-45 years of age) with newly diagnosed acute lymphoblastic leukaemia (ALL). EUDRACT number: 2018-001795-38.
- 18 Czepulkowski B: Basic techniques for the preparation and analysis of chromosomes from bone marrow and leukaemic blood. In: *Human cytogenetics: malignancy and acquired abnormalities*. Rooney DE (ed.). Oxford University Press, New York, pp. 1-26, 2001.
- 19 Czepulkowski B and Gibbons B: Cytogenetics in acute lymphoblastic leukaemia. In: *Human cytogenetics: malignancy and acquired abnormalities*. Rooney DE (ed.). Oxford University Press, New York, pp. 57-86, 2001.
- 20 McGowan-Jordan J, Hastings RJ and Moore S: *ISCN 2020: An International system for human cytogenomic nomenclature*. Basel, Karger, pp. 164, 2020.
- 21 Schroeder A, Mueller O, Stocker S, Salowsky R, Leiber M, Gassmann M, Lightfoot S, Menzel W, Granzow M and Ragg T: The RIN: an RNA integrity number for assigning integrity values to RNA measurements. *BMC Mol Biol* 7: 3, 2006. PMID: 16448564. DOI: 10.1186/1471-2199-7-3
- 22 Torkildsen S, Brunetti M, Gorunova L, Spetalen S, Beiske K, Heim S and Panagopoulos I: Rearrangement of the chromatin organizer special AT-rich binding protein 1 gene, *SATB1*, resulting from a t(3;5)(p24;q14) chromosomal translocation in acute myeloid leukemia. *Anticancer Res* 37(2): 693-698, 2017. PMID: 28179318. DOI: 10.21873/anticancer.11365
- 23 Panagopoulos I, Andersen K, Ramslien LF, Ikonomou IM, Micci F and Heim S: Therapy-related myeloid leukemia with the translocation t(8;19)(p11;q13) leading to a *KAT6A-LEUTX* fusion gene. *Anticancer Res* 41(4): 1753-1760, 2021. PMID: 33813379. DOI: 10.21873/anticancer.14940
- 24 Nicorici D, Satalan H, Edgren H, Kangaspeska S, Murumagi A, Kallioniemi O, Virtanen S and Kikku O: FusionCatcher - a tool for finding somatic fusion genes in paired-end RNA-sequencing data. *bioRxiv*, 2014. DOI: 10.1101/011650
- 25 Panagopoulos I, Gorunova L, Lund-Iversen M, Bassarova A and Heim S: Fusion of the genes *PHF1* and *TFE3* in malignant chondroid syringoma. *Cancer Genomics Proteomics* 16(5): 345-351, 2019. PMID: 31467228. DOI: 10.21873/cgp.20139
- 26 Panagopoulos I, Gorunova L, Andersen K, Lund-Iversen M, Lobmaier I, Micci F and Heim S: *NDRG1-PLAG1* and *TRPS1-PLAG1* fusion genes in chondroid syringoma. *Cancer Genomics Proteomics* 17(3): 237-248, 2020. PMID: 32345665. DOI: 10.21873/cgp.20184
- 27 Altschul SF, Gish W, Miller W, Myers EW and Lipman DJ: Basic local alignment search tool. *J Mol Biol* 215(3): 403-410, 1990. PMID: 2231712. DOI: 10.1016/S0022-2836(05)80360-2
- 28 Kent WJ: BLAT—the BLAST-like alignment tool. *Genome Res* 12(4): 656-664, 2002. PMID: 11932250. DOI: 10.1101/gr.229202
- 29 Kent WJ, Sugnet CW, Furey TS, Roskin KM, Pringle TH, Zahler AM and Haussler D: The human genome browser at UCSC. *Genome Res* 12(6): 996-1006, 2002. PMID: 12045153. DOI: 10.1101/gr.229102
- 30 Roohi J, Cammer M, Montagna C and Hatchwell E: An improved method for generating BAC DNA suitable for FISH. *Cytogenet Genome Res* 121(1): 7-9, 2008. PMID: 18544919. DOI: 10.1159/000124374
- 31 Panagopoulos I, Gorunova L, Andersen K, Lund-Iversen M, Hognestad HR, Lobmaier I, Micci F and Heim S: Chromosomal translocation t(5;12)(p13;q14) leading to fusion of high-mobility group AT-hook 2 gene with intergenic sequences from

- chromosome sub-band 5p13.2 in benign myoid neoplasms of the breast: a second case. *Cancer Genomics Proteomics* 19(4): 445-455, 2022. PMID: 35732319. DOI: 10.21873/cgp.20331
- 32 Panagopoulos I, Andersen K, Gorunova L, Davidson B, Micci F and Heim S: A novel cryptic t(2;3)(p21;q25) translocation fuses the *WWTR1* and *PRKCE* genes in uterine leiomyoma with 3q- as the sole visible chromosome abnormality. *Cancer Genomics Proteomics* 19(5): 636-646, 2022. PMID: 35985686. DOI: 10.21873/cgp.20348
- 33 Mitelman F, Johansson B and Mertens F: Mitelman Database of Chromosome Aberrations and Gene Fusions in Cancer. Available at: <https://mitelmandatabase.isb-cgc.org/> [Last accessed on November 22, 2022]
- 34 Paulsson K and Johansson B: Trisomy 8 as the sole chromosomal aberration in acute myeloid leukemia and myelodysplastic syndromes. *Pathol Biol (Paris)* 55(1): 37-48, 2007. PMID: 16697122. DOI: 10.1016/j.patbio.2006.04.007
- 35 Hemsing AL, Hovland R, Tsykunova G and Reikvam H: Trisomy 8 in acute myeloid leukemia. *Expert Rev Hematol* 12(11): 947-958, 2019. PMID: 31422708. DOI: 10.1080/17474086.2019.1657400
- 36 Taira T, Maeda J, Onishi T, Kitaura H, Yoshida S, Kato H, Ikeda M, Tamai K, Iguchi-Ariga SM and Ariga H: AMY-1, a novel C-MYC binding protein that stimulates transcription activity of C-MYC. *Genes Cells* 3(8): 549-565, 1998. PMID: 9797456. DOI: 10.1046/j.1365-2443.1998.00206.x
- 37 Furusawa M, Ohnishi T, Taira T, Iguchi-Ariga SM and Ariga H: AMY-1, a c-Myc-binding protein, is localized in the mitochondria of sperm by association with S-AKAP84, an anchor protein of cAMP-dependent protein kinase. *J Biol Chem* 276(39): 36647-36651, 2001. PMID: 11483602. DOI: 10.1074/jbc.M103885200
- 38 Furusawa M, Taira T, Iguchi-Ariga SM and Ariga H: AMY-1 interacts with S-AKAP84 and AKAP95 in the cytoplasm and the nucleus, respectively, and inhibits cAMP-dependent protein kinase activity by preventing binding of its catalytic subunit to A-kinase-anchoring protein (AKAP) complex. *J Biol Chem* 277(52): 50885-50892, 2002. PMID: 12414807. DOI: 10.1074/jbc.M206387200
- 39 Ishizaki R, Shin HW, Iguchi-Ariga SM, Ariga H and Nakayama K: AMY-1 (associate of Myc-1) localization to the trans-Golgi network through interacting with BIG2, a guanine-nucleotide exchange factor for ADP-ribosylation factors. *Genes Cells* 11(8): 949-959, 2006. PMID: 16866877. DOI: 10.1111/j.1365-2443.2006.00991.x
- 40 Jung HC and Kim K: Identification of MYCBP as a beta-catenin/LEF-1 target using DNA microarray analysis. *Life Sci* 77(11): 1249-1262, 2005. PMID: 15979100. DOI: 10.1016/j.lfs.2005.02.009
- 41 Waterman ML, Fischer WH and Jones KA: A thymus-specific member of the HMG protein family regulates the human T cell receptor C alpha enhancer. *Genes Dev* 5(4): 656-669, 1991. PMID: 2010090. DOI: 10.1101/gad.5.4.656
- 42 van Genderen C, Okamura RM, Fariñas I, Quo RG, Parslow TG, Bruhn L and Grosschedl R: Development of several organs that require inductive epithelial-mesenchymal interactions is impaired in LEF-1-deficient mice. *Genes Dev* 8(22): 2691-2703, 1994. PMID: 7958926. DOI: 10.1101/gad.8.22.2691
- 43 Lehrer S, Rheinstein PH and Rosenzweig KE: Loss of MycBP may be associated with the improved survival in 1P co-deletion of lower grade glioma patients. *Clin Neurol Neurosurg* 172: 112-115, 2018. PMID: 29986195. DOI: 10.1016/j.clineuro.2018.07.003
- 44 Li C, Tan F, Pei Q, Zhou Z, Zhou Y, Zhang L, Wang D and Pei H: Non-coding RNA MFI2-AS1 promotes colorectal cancer cell proliferation, migration and invasion through miR-574-5p/MYCBP axis. *Cell Prolif* 52(4): e12632, 2019. PMID: 31094023. DOI: 10.1111/cpr.12632
- 45 Wang A, Zhang T, Wei W, Wang H, Zhang Z, Yang W, Xia W, Mao Q, Xu L, Jiang F and Dong G: The long noncoding RNA *LINC00665* facilitates c-Myc transcriptional activity via the miR-195-5p MYCBP axis to promote progression of lung adenocarcinoma. *Front Oncol* 11: 666551, 2021. PMID: 34277412. DOI: 10.3389/fonc.2021.666551
- 46 Mintz L, Galperin E, Pasmanik-Chor M, Tulzinsky S, Bromberg Y, Kozak CA, Joyner A, Fein A and Horowitz M: EHD1 – an EH-domain-containing protein with a specific expression pattern. *Genomics* 59(1): 66-76, 1999. PMID: 10395801. DOI: 10.1006/geno.1999.5800
- 47 Pohl U, Smith JS, Tachibana I, Ueki K, Lee HK, Ramaswamy S, Wu Q, Mohrenweiser HW, Jenkins RB and Louis DN: EHD2, EHD3, and EHD4 encode novel members of a highly conserved family of EH domain-containing proteins. *Genomics* 63(2): 255-262, 2000. PMID: 10673336. DOI: 10.1006/geno.1999.6087
- 48 Naslavsky N and Caplan S: C-terminal EH-domain-containing proteins: consensus for a role in endocytic trafficking, EH? *J Cell Sci* 118(Pt 18): 4093-4101, 2005. PMID: 16155252. DOI: 10.1242/jcs.02595
- 49 Naslavsky N and Caplan S: EHD proteins: key conductors of endocytic transport. *Trends Cell Biol* 21(2): 122-131, 2011. PMID: 21067929. DOI: 10.1016/j.tcb.2010.10.003
- 50 Simone LC, Naslavsky N and Caplan S: Scratching the surface: actin' and other roles for the C-terminal Eps15 homology domain protein, EHD2. *Histol Histopathol* 29(3): 285-292, 2014. PMID: 24347515. DOI: 10.14670/HH-29.285
- 51 Guilherme A, Soriano NA, Bose S, Holik J, Bose A, Pomerleau DP, Furcinitti P, Leszyk J, Corvera S and Czech MP: EHD2 and the novel EH domain binding protein EHBP1 couple endocytosis to the actin cytoskeleton. *J Biol Chem* 279(11): 10593-10605, 2004. PMID: 14676205. DOI: 10.1074/jbc.M307702200
- 52 George M, Ying G, Rainey MA, Solomon A, Parikh PT, Gao Q, Band V and Band H: Shared as well as distinct roles of EHD proteins revealed by biochemical and functional comparisons in mammalian cells and *C. elegans*. *BMC Cell Biol* 8: 3, 2007. PMID: 17233914. DOI: 10.1186/1471-2121-8-3
- 53 Doherty KR, Demonbreun AR, Wallace GQ, Cave A, Posey AD, Heretis K, Pytel P and McNally EM: The endocytic recycling protein EHD2 interacts with myoferlin to regulate myoblast fusion. *J Biol Chem* 283(29): 20252-20260, 2008. PMID: 18502764. DOI: 10.1074/jbc.M802306200
- 54 Benjamin S, Weidberg H, Rapaport D, Pekar O, Nudelman M, Segal D, Hirschberg K, Katrav S, Ehrlich M and Horowitz M: EHD2 mediates trafficking from the plasma membrane by modulating Rac1 activity. *Biochem J* 439(3): 433-442, 2011. PMID: 21756249. DOI: 10.1042/BJ20111010
- 55 Pekar O, Benjamin S, Weidberg H, Smaldone S, Ramirez F and Horowitz M: EHD2 shuttles to the nucleus and represses transcription. *Biochem J* 444(3): 383-394, 2012. PMID: 22448906. DOI: 10.1042/BJ20111268
- 56 Horton P and Nakai K: Better prediction of protein cellular localization sites with the k nearest neighbors classifier. *Proc Int Conf Intell Syst Mol Biol* 5: 147-152, 1997. PMID: 9322029.

- 57 Thumhuri V, Almagro Armenteros JJ, Johansen AR, Nielsen H and Winther O: DeepLoc 2.0: multi-label subcellular localization prediction using protein language models. *Nucleic Acids Res* 50(*W1*): W228-W234, 2022. PMID: 35489069. DOI: 10.1093/nar/gkac278
- 58 Miyoshi H, Ohira M, Shimizu K, Mitani K, Hirai H, Imai T, Yokoyama K, Soeda E and Ohki M: Alternative splicing and genomic structure of the AML1 gene involved in acute myeloid leukemia. *Nucleic Acids Res* 23(*14*): 2762-2769, 1995. PMID: 7651838. DOI: 10.1093/nar/23.14.2762
- 59 Ghozi MC, Bernstein Y, Negreanu V, Levanon D and Groner Y: Expression of the human acute myeloid leukemia gene *AML1* is regulated by two promoter regions. *Proc Natl Acad Sci USA* 93(*5*): 1935-1940, 1996. PMID: 8700862. DOI: 10.1073/pnas.93.5.1935
- 60 Martinez M, Hinojosa M, Trombly D, Morin V, Stein J, Stein G, Javed A and Gutierrez SE: Transcriptional auto-regulation of *RUNX1* P1 promoter. *PLoS One* 11(*2*): e0149119, 2016. PMID: 26901859. DOI: 10.1371/journal.pone.0149119
- 61 Levanon D, Bernstein Y, Negreanu V, Ghozi MC, Bar-Am I, Aloya R, Goldenberg D, Lotem J and Groner Y: A large variety of alternatively spliced and differentially expressed mRNAs are encoded by the human acute myeloid leukemia gene *AML1*. *DNA Cell Biol* 15(*3*): 175-185, 1996. PMID: 8634147. DOI: 10.1089/dna.1996.15.175
- 62 Telfer JC and Rothenberg EV: Expression and function of a stem cell promoter for the murine *CBFalpha2* gene: distinct roles and regulation in natural killer and T cell development. *Dev Biol* 229(*2*): 363-382, 2001. PMID: 11203699. DOI: 10.1006/dbio.2000.9991
- 63 Fujita Y, Nishimura M, Taniwaki M, Abe T and Okuda T: Identification of an alternatively spliced form of the mouse *AML1/RUNX1* gene transcript AML1c and its expression in early hematopoietic development. *Biochem Biophys Res Commun* 281(*5*): 1248-1255, 2001. PMID: 11243869. DOI: 10.1006/bbrc.2001.4513
- 64 Pozner A, Lotem J, Xiao C, Goldenberg D, Brenner O, Negreanu V, Levanon D and Groner Y: Developmentally regulated promoter-switch transcriptionally controls *Runx1* function during embryonic hematopoiesis. *BMC Dev Biol* 7: 84, 2007. PMID: 17626615. DOI: 10.1186/1471-213X-7-84
- 65 Sroczyńska P, Lancrin C, Kouskoff V and Lacaud G: The differential activities of *Runx1* promoters define milestones during embryonic hematopoiesis. *Blood* 114(*26*): 5279-5289, 2009. PMID: 19858498. DOI: 10.1182/blood-2009-05-222307
- 66 Medina MA, Ugarte GD, Vargas MF, Avila ME, Necuñir D, Elorza AA, Gutiérrez SE and De Ferrari GV: Alternative *RUNX1* promoter regulation by Wnt/ β -catenin signaling in leukemia cells and human hematopoietic progenitors. *J Cell Physiol* 231(*7*): 1460-1467, 2016. PMID: 26580584. DOI: 10.1002/jcp.25258
- 67 Zhou TH, Su JZ, Qin R, Chen X, Ju GD and Miao S: Prognostic and predictive value of a 15 transcription factors (TFs) panel for hepatocellular carcinoma. *Cancer Manag Res* 12: 12349-12361, 2020. PMID: 33293862. DOI: 10.2147/CMAR.S279194
- 68 Takeuchi Y, Yoshida K, Halik A, Kunitz A, Suzuki H, Kakiuchi N, Shiozawa Y, Yokoyama A, Inoue Y, Hirano T, Yoshizato T, Aoki K, Fujii Y, Nannya Y, Makishima H, Pfitzner BM, Bullinger L, Hirata M, Jinnouchi K, Shiraiishi Y, Chiba K, Tanaka H, Miyano S, Okamoto T, Haga H, Ogawa S and Damm F: The landscape of genetic aberrations in myxofibrosarcoma. *Int J Cancer* 151(*4*): 565-577, 2022. PMID: 35484982. DOI: 10.1002/ijc.34051

Received November 3, 2022
Revised November 16, 2022
Accepted November 23, 2022